Mechanism of Binding of NO to Soluble Guanylyl Cyclase: Implication for the Second NO Binding to the Heme Proximal Site

ARTICLE *in* BIOCHEMISTRY · MARCH 2012

Impact Factor: 3.02 · DOI: 10.1021/bi300105s · Source: PubMed

4 AUTHORS, INCLUDING:

Emil Martin
University of Texas Medical School
62 PUBLICATIONS **2,637** CITATIONS
SEE PROFILE

Iraida Sharina
University of Texas Medical School
40 PUBLICATIONS **604** CITATIONS
SEE PROFILE

Ah-Lim Tsai
University of Texas Health Science Center at H…
142 PUBLICATIONS **4,614** CITATIONS
SEE PROFILE

BIOCHEMISTRY
including biophysical chemistry & molecular biology

Article

pubs.acs.org/biochemistry

Mechanism of Binding of NO to Soluble Guanylyl Cyclase: Implication for the Second NO Binding to the Heme Proximal Site

Emil Martin,*[,†] Vladimir Berka,[‡] Iraida Sharina,[†] and Ah-Lim Tsai*[,‡]

[†]Division of Cardiology, Internal Medicine, The University of Texas Medical School at Houston, Houston, Texas 77030, United States

[‡]Division of Hematology, Internal Medicine, The University of Texas Medical School at Houston, Houston, Texas 77030, United States

Supporting Information

ABSTRACT: Soluble guanylyl cyclase (sGC), the key enzyme for the formation of second messenger cyclic GMP, is an authentic sensor for nitric oxide (NO). Binding of NO to sGC leads to strong activation of the enzyme activity. Multiple molecules and steps of binding of NO to sGC have been implicated, but the target of the second NO and the detailed binding mechanism remain controversial. In this study, we used ^{15}NO and ^{14}NO and anaerobic sequential mixing−freeze-quench electron paramagnetic resonance to unambiguously confirm that the heme Fe is the target of the second NO. The linear dependence on NO concentration up to 600 s^{-1} for the observed rate of the second step of NO binding not only indicates that the binding site of the second NO is different from that in the first step, i.e., the proximal site of the heme, but also supports a concerted mechanism in which the dissociation of the His105 proximal ligand occurs simultaneously with the binding of the second NO molecule. Computer modeling successfully predicts the kinetics of formation of a set of five-coordinate NO complexes with the ligand on either the distal or proximal site and supports the selective release of NO from the distal side of the transient bis-NO−sGC complex. Thus, as has been demonstrated with cytochrome *c*′, a five-coordinate NO−sGC complex containing a proximal NO is formed after the binding of the second NO.

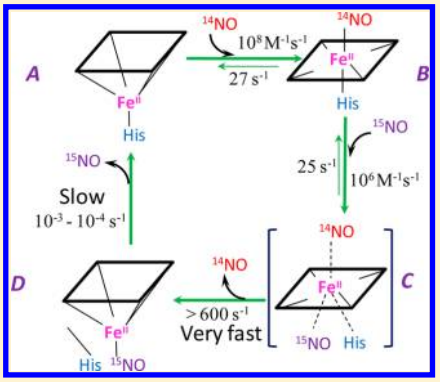

Mammalian soluble guanylyl cyclase (sGC) is an authentic heme-based sensor for nitric oxide (NO). The catalytic center of sGC is formed by the C-terminal halves of both α and β subunits, while the heme center is located in the N-terminal domain of the β subunit. Resting sGC has a five-coordinate (5c) ferrous heme [Fe(II)] containing a proximal histidine ligand (His105).[1] Binding of NO to the heme center increases its basal activity for catalytic conversion from GTP to cyclic GMP by several hundred-fold.[2,3] sGC does not bind oxygen but binds carbon monoxide (CO), which causes an only few-fold increase in activity. Binding of CO to sGC differs from binding of NO in three aspects. (1) CO binds sGC as a single reversible step, while NO binds sGC as a multiple and overall irreversible process with an apparent K_D on the picomolar level.[4] (2) Binding of CO to sGC forms a stable six-coordinate (6c) complex, while NO binding causes dissociation of the proximal histidine ligand to form a five-coordinate (5c) NO−sGC complex. (3) Only one molecule of CO binds to sGC, but two molecules of NO bind to sGC sequentially; both the first step, formation of a 6c NO complex, and the second step, further conversion to a 5c NO complex, exhibit NO concentration dependence.[4]

The binding site of the second NO has not been determined. It was postulated to bind to the sGC heme iron as a proximal ligand by displacing the original histidine ligand, His105, similar to that demonstrated for cytochrome *c*′ by mutagenesis and crystallographic analysis.[5,6] An alternative proposal for the binding site of the second NO during the activation process is a cysteine thiol, or at a non-heme site.[7−11] However, nitrosation of cysteine does not occur in the absence of oxygen, and even in the presence of oxygen, the reaction is too slow to contribute to the observed fast NO binding.[12,13] As no evidence indicates an additional metal center near the heme iron that could be a second NO target, it is more plausible to test the idea of heme as the binding site for the second NO molecule as represented by Scheme 1 (A ↔ B ↔ C). On the basis of the observed NO concentration dependence of the B ↔ C conversion, the second molecule of NO has to bind to the heme to cause spectral changes, and this site cannot be the distal site of the heme; otherwise, NO concentration dependence would not be observed. It is only logical to assume that the second NO targets the proximal side of the heme iron, to form a transient bis-NO−sGC complex, Fe(II)$(NO)_2$ (or a quaternary transition complex, C, in Scheme 1), which then transforms further into a stable 5c NO complex, 5pFe(II)NO (B ↔ C → D in Scheme 1). However, there is no direct evidence of whether the remaining heme-bound NO ligand comes from the second molecule of NO and whether this ligand is at the distal or

Received: January 23, 2012
Revised: March 7, 2012
Published: March 8, 2012

   dx.doi.org/10.1021/bi300105s | *Biochemistry* 2012, 51, 2737−2746

Scheme 1. Reaction between NO and sGC[a]

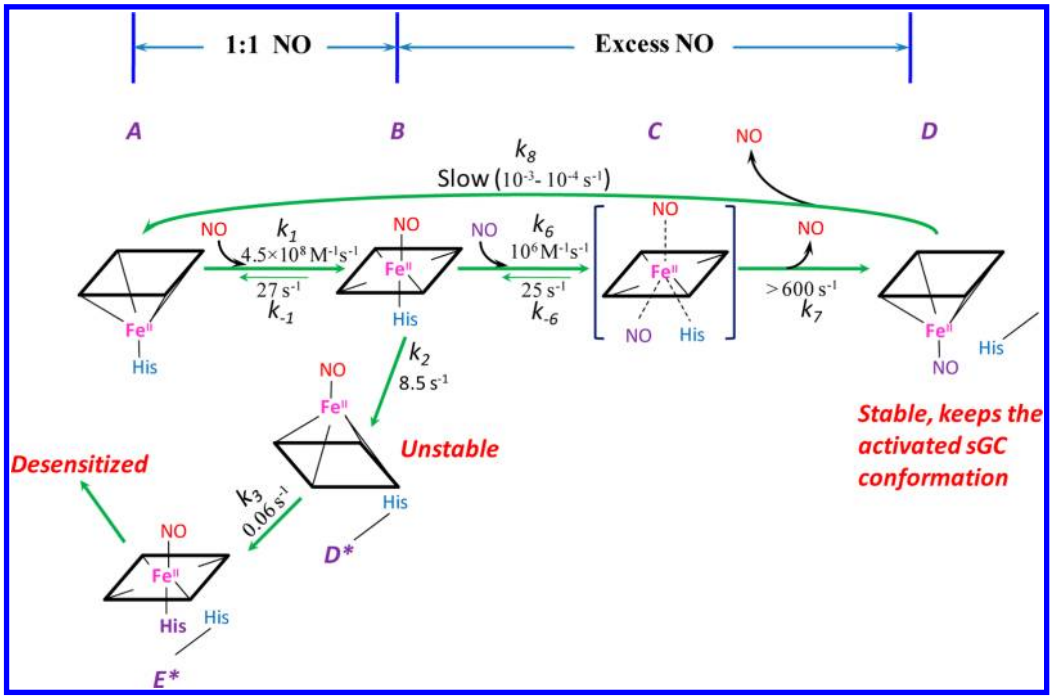

[a]Species A–D, D*, and E* are identified by rapid-scan UV–vis spectroscopic and EPR under stoichiometric and excess amounts of NO. Rate constants for each chemical step were determined by us at 24 °C except the slow dissociation from D to A, for which measurements from literature were used.[27,28] The reactions with stoichiometric NO, A ↔ B → D* → E* → desensitized sGC, are a simplified version as compared to Table 1, whereas the cycling from B back to A was measured when 1 mM CO and 25 mM dithionite were added at the time of maximal formation of B.[19] The proximal histidine ligand (purple) denotes an alternative histidine, likely His107.

proximal side of the heme. We would like to resolve these key issues to fully understand the interaction between NO and sGC and the coupling between NO binding and sGC activation.

To confirm if heme is the target of the second NO and to demonstrate that the second NO binds to the proximal site of the heme, we used ^{15}NO and ^{14}NO as heme ligand structural probes for the two NO binding steps in combination with sequential stopped-flow and freeze-quench EPR and followed the kinetics of multiple steps of binding of NO to sGC. We took advantage of the power of EPR in discriminating between isotopic NO–sGC binding complexes and succeeded in generating unambiguous answers for the key questions raised above and also derived a unified mechanistic model regarding the interaction between NO and sGC.

MATERIALS AND METHODS

Protein Expression and Purification. The sGC enzyme was expressed in Sf9 cells and purified by anion-exchange and affinity chromatography as detailed previously.[13] The sample was supplemented with 1 mM $MgCl_2$ and stored at −80 °C in 25% glycerol. The preparations were at least 95% pure as judged by sodium dodecyl sulfate–polyacrylamide gel electrophoresis with Coomasie Blue staining and immunoblotting. The anaerobic sGC sample was prepared in a glass tonometer via a five-cycle vacuum (30 s) argon replacement (5 min) on an anaerobic train.

Preparation of NO Solutions. A ^{14}NO solution was prepared using the 99.9% pure ^{14}NO gas, which was further cleaned up from degradation products by being passed through a U-shaped tube filled with dry KOH pellets. Anaerobic 50 mM triethanolamine (TEA, pH 7.4) buffer prepared via nitrogen purging for 10 min was bubbled for an additional 10 min with purified ^{14}NO to obtain an ∼2 mM solution. The solution was kept in a gastight glass tonometer and stored in an anaerobic chamber (Coy Laboratory Products, Inc.). The stock solution of ^{15}NO (Cambridge Isotope Laboratories, Andover, MA) was prepared similarly. The exact concentration of NO in the stock solution was determined using an oxyhemoglobin (HbO_2) assay.[14] Working NO solutions of different concentrations were prepared by adding the necessary amount of NO stock to a plastic gastight syringe containing anaerobic 50 mM TEA (pH 7.4) and used immediately for measurements.

Monitoring of Formation of the sGC–NO Complex. The dynamics of formation of the sGC–NO complex was monitored at room temperature (24 °C) in the anaerobic chamber, using a Bio-SEQUENTIAL DX-18MV stopped-flow instrument (Applied Photophysics, Leatherhead, U.K.). The time-dependent UV–vis spectra and single-wavelength kinetic data were recorded with a rapid-scan photodiode array detector at a rate of 400 scans/s for up to 1 s and with a single-wavelength mode of the stopped flow, respectively. We always found a good match in kinetics and amplitude change at each wavelength in both rapid-scan and single-wavelength mode, indicating minimal extra photodissociation or photodecomposition of any intermediates caused by the stronger light intensity in the rapid-scan measurements.

Trapping sGC–NO Complexes by Freeze Quench. Single-stage rapid-freeze quench (RFQ) at 24 °C was performed using our Update Instrument (Madison, WI) System 1000 located in an anaerobic chamber and prechilled isopentane as previously described.[15,16]

To freeze trap different intermediates of the NO–sGC reaction with two-stage mixing, we prepared sGC–NO complexes using the same anaerobic sequential stopped flow

dx.doi.org/10.1021/bi300105s | Biochemistry 2012, 51, 2737–2746

Table 1. Reaction Steps and Rate Constants for the NO Binding Mechanism of sGC

reaction step	terms in Scheme 1	rate constant	value[a]
5cFe(II) + NO ↔ 6cFe(II)NO	A ↔ B	k_1/k_{-1}	4.5×10^8 M^{-1} s^{-1}/27 s^{-1}
6cFe(II)NO ↔ 5cFe(II)NO[b]	B ↔ D*	k_2/k_{-2}	8.5 s^{-1}/0.001 s^{-1}
5cFe(II)NO ↔ 6cxFe(II)NO[b]	D* ↔ E*	k_3/k_{-3}	0.06 s^{-1}/0 s^{-1}
6cxFe(II)NO ↔ 5cxFe(II)[b]		k_4/k_{-4}	2 s^{-1}/0 s^{-1}
5cxFe(II) ↔ 5cFe(II)NO[b]		k_5/k_{-5}	0.006 s^{-1}/0 s^{-1}
6cFe(II)NO + NO ↔ Fe(II)$(NO)_2$	B ↔ C	k_6/k_{-6}	1.1×10^6 M^{-1} $^{-1}$/25 s^{-1}
Fe(II)$(NO)_2$ ↔ 5pFe(II)NO	C ↔ D	k_7/k_{-7}	1000 s^{-1}/0 s^{-1}
5pFe(II)NO ↔ 5cFe(II) + NO	D ↔ A	k_8/k_{-8}	0.0001 s^{-1}/0 s^{-1}

[a]Values are those determined at 24 °C as we previously reported[13,26] or determined recently for a stoichiometric or excess amount of NO.[19,20] [b]Steps observed only when the sGC:NO ratio is 1:1. The k_4/k_{-4} and k_5/k_{-5} steps are not included in Scheme 1.

and an open-ended flow cell controlled by a double-push program. Two knurled-screw plungers of the instrument were preset to deliver equal volumes of reactants with each push. In the first push, 9 μM sGC sample was mixed with an equal volume of 10 μM ^{14}NO and incubated in the aging loop of the stopped-flow instrument for 20 ms. With the second push, the preformed sGC−^{14}NO complex was mixed with equal volumes of 5 or 50 μM ^{15}NO and displaced from the system by 50 mM TEA (pH 7.4). The samples were captured in an EPR tube and immediately plunged into a dry ice/ethanol bath (−30 °C). It took 5−10 s to completely freeze the sample in the 5 mm EPR tube. Subsequently, the sample was transferred from the anaerobic chamber to liquid nitrogen. In some control experiments, the second NO solution was replaced by buffer. In other experiments, sGC was first reacted with a ^{15}NO solution, followed by a second mixing with ^{14}NO.

Such a freeze-quench experimental arrangement allows for acquisition and direct comparison of both optical and EPR data from identical samples. It also avoids the packing factor of the rapid freeze in isopentane that adds another ∼2-fold dilution and heterogeneity of the final packed sample in our rapid-freeze instrument.

EPR Spectroscopy. Liquid nitrogen-temperature EPR spectra were recorded with a Bruker EMX spectrometer using a BVT3000 temperature controller and a silver-coated double-jacketed glass transfer line.[17] The conditions for EPR measurements at 110 K were as follows: frequency, 9.2 GHz; modulation amplitude, 2 G; modulation frequency, 100 kHz; time constant, 0.33 s.

Mathematical Modeling. Numerical integration to simulate the NO complex intermediates, especially the 5c NO−sGC intermediates, was conducted using the feature of a kinetic block, containing all the chemical steps as listed in Table 1 (Scheme 1) and the rate constants determined by us at 24 °C, in SCoP (Simulation Resources Inc., Redlands, CA), as we reported previously.[18,19]

RESULTS AND DISCUSSION

Heme Is the Binding Site of the Second NO Molecule. Our first goal was to confirm that the heme is the target of the second NO. For this purpose, we used symmetric sequential-mixing stopped flow of sGC with NO solutions containing different nitrogen isotopes in the two reaction stages. Such kinetic measurement led to 2-fold dilution in the first mixing and another 2-fold dilution in the second mixing.[20] To avoid any confusion about the sample concentrations, all values presented here are the starting concentrations "before" mixing, unless indicated otherwise.

Before conducting the freeze trap EPR kinetic experiments using isotopic NO, we ran parallel optical kinetic measurements to optimize the aging time of the sequential mixing. A one-stage mixing rapid-scan measurement of the anaerobic reaction between ∼7 μM sGC and 7 μM NO showed a 420 nm intermediate that peaked at 1.5 ms, mainly the 6c NO−sGC complex [or 6cFe(II)NO in Table 1] (Figure 1A). The very fast first step, conversion from the resting ferrous sGC, with a Soret peak at 432 nm, to the 6c NO−sGC complex, was totally complete within the 1.5 ms dead time of our stopped-flow instrument. This intermediate transformed within 1 s further to a species with a 399 nm peak, the 5c NO−sGC complex [or 5cFe(II)NO in Table 1] with an isosbestic point at 405 nm (Figure 1A), seemingly indicating that only one chemical step was involved, consistent with previous observations.[4,13] Our recent study indicates that the first step of binding of NO to sGC has an association rate constant (k_1) of 4.5×10^8 M^{-1} s^{-1} and a dissociation rate constant (k_{-1}) of 27 s^{-1} at 24 °C (Table 1 and ref 19). As estimated by the 420 nm amplitude at 20 ms, ∼80% of the enzyme was present as the 6c NO−sGC complex (Figure 1A). The same amount of 6c NO−sGC complex was predicted by computer simulation (Figure 5A). The value of 20 ms was chosen as the minimal reliable aging time for our sequential stopped-flow instrument, and also the point at which the 6c NO−sGC complex is still the dominant sGC species before conversion to the 5c NO−sGC complex.

Transient formation of the 6c NO−sGC complex was also confirmed by one-stage rapid-freeze EPR measurements. As shown in Figure 1B, equal mixing of sGC and NO (10 μM each) followed by freeze trapping at 20 ms yielded an EPR spectrum consistent with a mixture of 6c rhombic and 5c axial low-spin NO−heme complex (spectrum **b**). In contrast, the sample freeze trapped ∼5 s after mixing showed a spectrum typical for 5c axial NO−heme complex (spectrum **a**) with $g_x = g_y = 2.076$ and $g_z = 2.008$ with a typical three-line hyperfine splitting (A_N = 17 G) caused by the nitrogen nucleus of NO. Arithmetic analysis with spectra a and b normalized to the same spin concentration indicated that the sample freeze trapped at 20 ms is dominated by the 6c NO−sGC complex, which accounts for ∼75% of the total sGC (spectrum **c**, which is the difference between spectrum **b** and 25% of spectrum **a**). The EPR spectrum of the resolved 6c NO−sGC complex was optimally simulated by rhombic NO heme with g values of 2.097, 2.018, and 1.985 and a nine-line (3 × 3) hyperfine pattern caused by nitrogen nuclei from NO (A_{N1} = 22 G) and the proximal histidine, H105 (A_{N2} = 6G) (spectrum **d**). Although a similar EPR result for the 6c NO−sGC complex was obtained by reaction of sGC with a NO releaser at −24 °C in a buffer containing 40% ethylene glycol and manual freezing,[21] the data shown in Figure 1B are the first obtained by RFQ EPR. Kinetically, the contribution of the 6c NO−sGC complex to the EPR data appears to match nicely with the optical kinetic data shown in Figure 1A and that predicted by computer modeling (Figure 5A).

dx.doi.org/10.1021/bi300105s | Biochemistry 2012, 51, 2737−2746

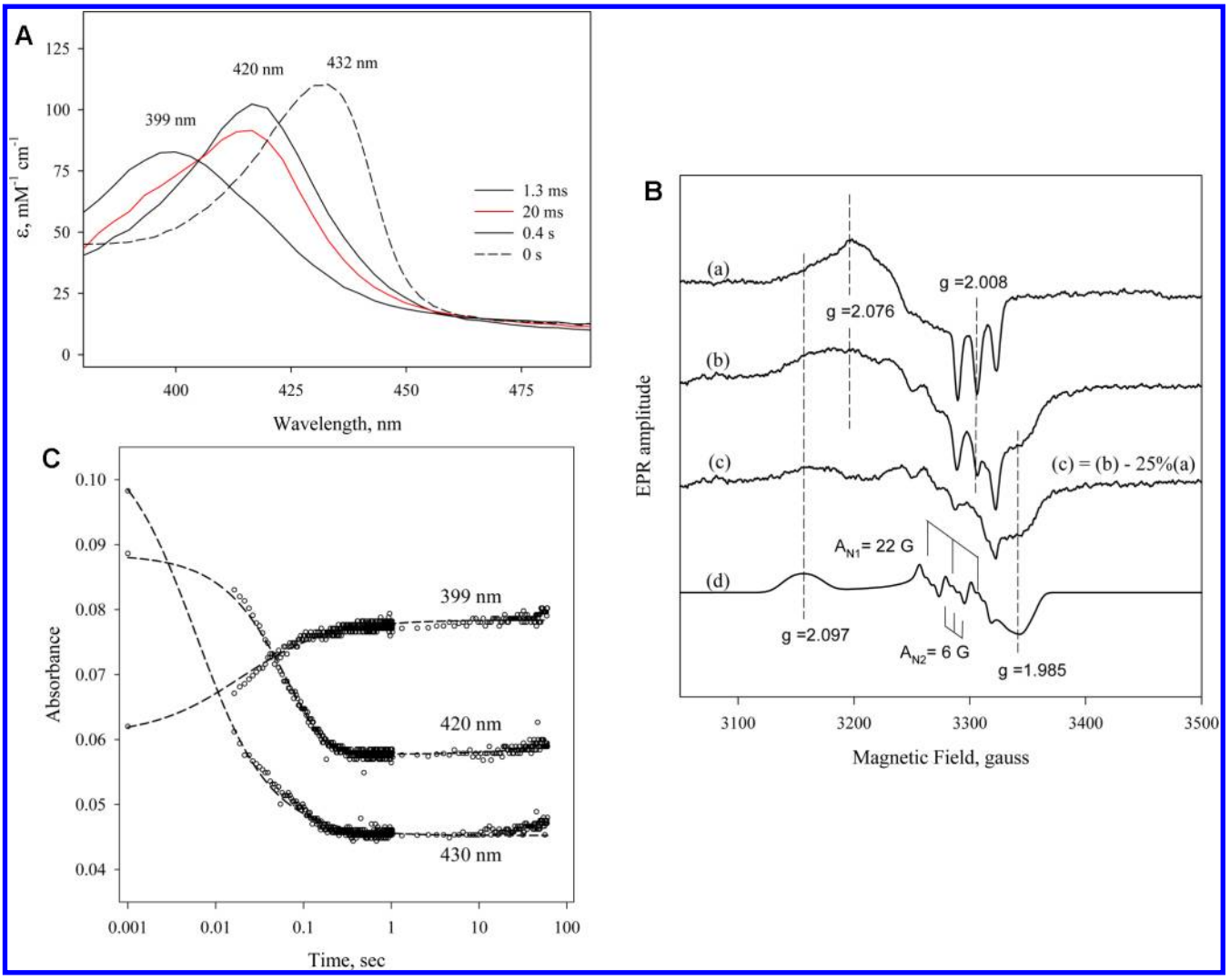

Figure 1. (A) Time-resolved spectra of the reaction between sGC and a stoichiometric amount of NO. NO binding reactions of sGC monitored by rapid-scan single mixing at 24 °C. The concentrations of both sGC and NO were 7 μM. Three spectra recorded at 1.3 ms, 20 ms, and 1.0 s of the 400 collected are shown. A matching resting Fe(II)sGC spectrum recorded on an HP8453 spectrophotometer is also shown as a "zero" time control (−−−). (B) Transient formation of the 6c NO−sGC complex identified by RFQ EPR kinetic measurement. sGC and NO (10 μM each) were reacted at 24 °C by single-stage equal mixing and freeze trapped with cold isopentane (113 K). The ram velocity was 1.25 cm/s, and the packing factor was 0.45.[16] The EPR spectra for samples trapped at 20 ms (b) and 5 s (a) are one out of three repeats, which show similar results. Spectrum **c** is the difference between spectrum **b** and 25% of spectrum **a**, which reveals the dominant 6c NO−sGC species. Simulation of the EPR of the 6c NO−sGC complex (spectrum **d**) was done by Simfonia as a frozen powder sample. Hyperfine splitting constants related to the nitrogen nuclei from NO, A_{N1}, and His105, A_{N2}, are indicated. Spectra a and b are averages of 32 scans. Key g values for the NO−sGC complexes are also indicated. (C) Kinetics of resting sGC (by A_{432}), the 6c NO−sGC complex (A_{420}), and the 5c NO−sGC complex (A_{399}) in the second-stage reaction of the anaerobic sequential stopped flow at 24 °C. The reaction in the first stage was between 5 μM sGC and 5 μM NO, and the mixture, after a 20 ms delay, was further reacted with 5 μM NO in the second mixing. Dashed lines are visual guides connecting all data points that are not evenly distributed on the logarithmic scale, especially those of <10 ms.

In the next step, we examined the kinetic change of different intermediates of NO−sGC interaction in a sequential mixing experiment. sGC (5 μM) was mixed with 5 μM NO during the first-stage mixing and aged for 20 ms and then reacted with additional 5 μM NO during the second-stage mixing. The disappearance of 6cFe(II)NO, monitored at 420 nm, and the formation of the 5c NO−sGC complex followed at 399 nm were fast and reached a plateau after ∼0.2 s (Figure 1C). The level of 6cFe(II)NO, the 5c NO−sGC complex, and even the 5c Fe(II)−sGC complex remained pretty much unchanged during the 0.5−60 s period after the second mixing (Figure 1C), indicating that the amount of all 5c sGC−NO species basically plateaued for a period of ≫10 s after the second mixing. This result also indicates that during the 1 min period after the second mixing there is not much cycling from the 5c NO−sGC complex back to the resting ferrous sGC to allow another cycle of NO interaction.

To trap various NO−sGC intermediates for EPR characterization, we generated the maximal amount of the 6c NO−sGC complex in the first-stage mixing of the sequential stopped flow, and after 20 ms, the reaction mixture was further mixed with the second NO with the opposite nitrogen isotope in the second stage. As the nuclear spins of ^{15}N and ^{14}N are $^1/_2$ and 1, respectively, we expected to see a very contrasting two-line (A_N ∼ 22 G for ^{15}NO) or three-line (A_N ∼ 17 G for ^{14}NO) z-hyperfine splitting pattern in the EPR of the 5c NO−sGC

dx.doi.org/10.1021/bi300105s | *Biochemistry* 2012, 51, 2737−2746

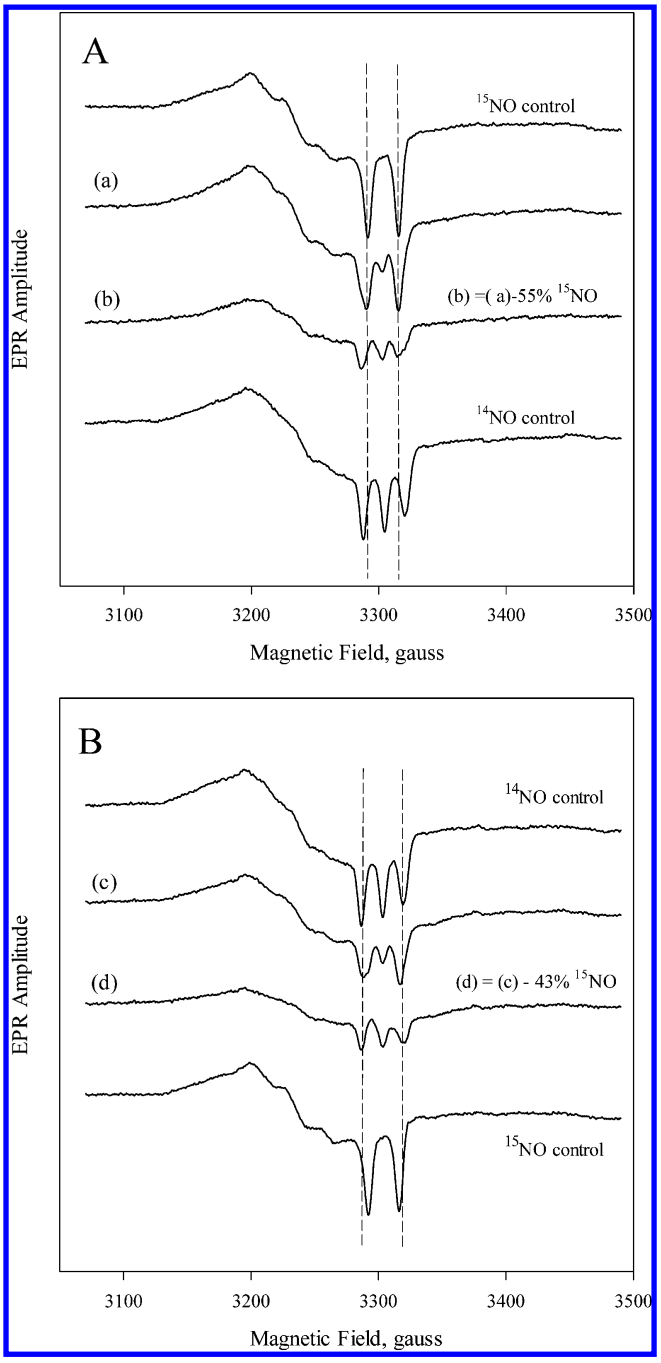

Figure 2. EPR spectra of sGC that reacted sequentially with a stoichiometric amount of ^{15}NO and ^{14}NO (A) or with a reverse sequence of the isotopic NO (B). The sequential stopped-flow and freeze trap procedure is detailed in Materials and Methods. The 20 ms aging time for the first mixing was used, and the sGC concentration was 9.0 μM for both experiments. (A) Isotopic NO ligand was used at concentrations of 10.0 and 5.0 μM in the first and second mixing, respectively. The ^{14}NO and ^{15}NO control spectra of the 5c NO−sGC complex generated from 9.0 μM sGC with an excess of individual isotopic NO and manually frozen after ∼10 s are shown as the top and bottom spectra, respectively. Spectrum **a** is the EPR spectrum of the freeze-trapped sample 5−10 s after the second mixing, and spectrum **b** is the difference spectrum between spectrum **a** and 55% of the ^{15}NO control. Spectrum **c** is equivalent to spectrum **a** in panel A, but with opposite isotopic NO sequence. Spectrum **d** is the difference between spectrum **c** and 43% of the ^{15}NO control. All spectra are normalized against their total spin concentration by double integration. The difference spectra (**b** and **d**) are the optimally resolved EPR spectra, containing the essentially pure spectrum of either ^{15}NO or ^{14}NO control EPR. This was achieved by serial arithmetic subtraction from the EPR of individual freeze-trapped samples (**b** or **d**) by different fractions of the control spectrum and visual comparison with either control spectrum. EPR conditions are described in Materials and Methods, and each spectrum is the average of 8−20 repetitive scans.

complex depending upon whether ^{15}NO or ^{14}NO is the remaining heme ligand. Combination of isotopic NO and EPR spectroscopy is probably a much more effective approach for following the identity of the heme-bound NO and its coordination site, either proximal or distal, in the first and second binding steps than other spectroscopic methods, such as resonance Raman or Mössbauer spectroscopy, considering signal resolution, sample usage, and ease of execution of the measurements.

The pure 5c ^{15}NO− and ^{14}NO−sGC control samples created by reaction of 9 μM sGC at 24 °C with an excess of either ^{15}NO or ^{14}NO display typical axial EPR spectra with prominent two-line and three-line hyperfine features, respectively, for the g_z component (Figure 2A, top and bottom control spectra). The EPR spectrum for the sample obtained by mixing 9 μM sGC first with 10 μM ^{15}NO and then with 5 μM ^{14}NO [(1:1):1 two-stage mixing] followed by freeze trapping for 5−10 s at −30 °C is shown in Figure 2A (spectrum **a**). This spectrum corresponds to the 5c NO−sGC complex containing a mixture of the ^{15}NO and ^{14}NO control spectra. Subtraction of 55% of the ^{15}NO control spectrum from the experimentally obtained spectrum **a** yields a difference EPR spectrum with a line shape essentially identical to that of the ^{14}NO control (Figure 2A, spectrum **b** vs the bottom spectrum).

In the second experiment, we reversed the order of the isotopic NO, i.e., 9 μM sGC first reacted with 10 μM ^{14}NO and then with 5 μM ^{15}NO [(1:1):1 two-stage mixing]. The EPR spectrum of the trapped sample was best expressed as a mixture of the 5c NO−sGC complex containing 57% ^{14}NO and 43% ^{15}NO (Figure 2B). Although the isotopic NO was swapped in this experiment, the isotope distribution is very similar to that in Figure 2A, indicating that the two isotopic NO ligands have the same binding behavior.

To see the effect of a modest excess of NO in the first mixing, we mixed 9 μM sGC with 15 μM ^{14}NO and aged the sample for 20 ms before further mixing it with 7.5 μM ^{15}NO and freeze trapping it [(1:1.6):1.6 two-stage mixing]. This sample gave a composite EPR spectrum (Figure 3A, spectrum **c**) that is best simulated as a mixture of 43% 5c ^{14}NO−sGC complex and 57% 5c ^{15}NO−sGC complex (Figure 3A, spectrum **d** vs the bottom spectrum). The amount of ^{15}NO remaining in the final sample was increased from the experiment with a (1:1):1 mixing scheme [i.e., 43% (Figure 2B)].

To test whether the ratio between the ^{15}NO− and ^{14}NO−sGC complexes can be substantially modulated by varying the concentration of the NO present in the second mixing, we first mixed 9 μM sGC with 10 μM ^{14}NO and aged it for 20 ms before further mixing it with 50 μM (i.e., 10 fold excess) ^{15}NO [(1:1):10 two-stage mixing] and freeze trapped the resulting sample. The EPR spectrum of this sample (Figure 3B, spectrum **e**) can be optimally simulated as a mixture of 15% ^{14}NO−sGC complex and 85% ^{15}NO−sGC complex (Figure 3B, spectrum **f**), indicating that we were able to enrich a specific isotope-

dx.doi.org/10.1021/bi300105s | *Biochemistry* 2012, 51, 2737−2746

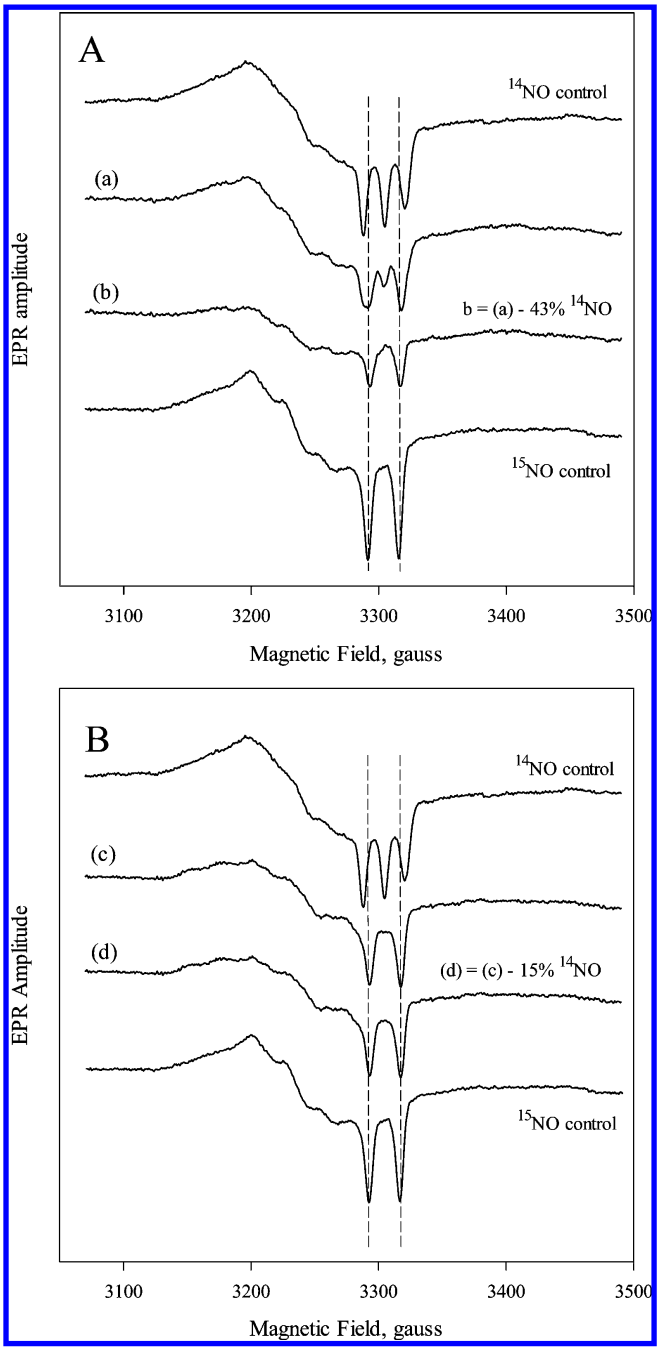

Figure 3. EPR spectra of the reaction of sGC (9.0 μM) with excess NO in either the first-stage (A) or second-stage (B) reaction of the sequential mixing experiments. (A) ^{14}NO (15 μM) and ^{15}NO (7.5 μM) were used in the first and second mixings, respectively. Spectrum **a** is the EPR spectrum of the freeze-trapped sample 5–10 s after the second mixing, and spectrum **b** is the difference spectrum between spectrum **a** and 43% of that of the ^{14}NO control. (B) Similar to A, but 10 μM ^{14}NO and 50 μM ^{15}NO were used in the first and second mixings, respectively. Spectrum **c** is the EPR spectrum of the freeze-trapped sample, and spectrum **d** is the difference spectrum between spectrum **c** and 15% of that of the ^{14}NO control.

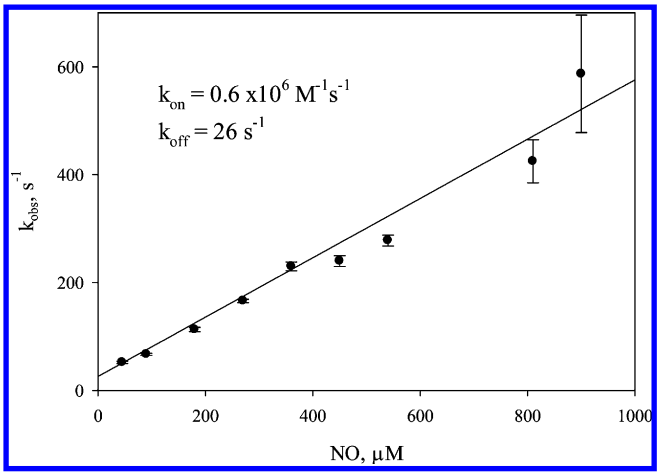

Figure 4. NO concentration dependence of the observed rate for the second-step binding of NO to sGC. sGC (2 μM) was mixed with eight different levels of NO ranging from 90 to 1800 μM in the anaerobic stopped flow, and the kinetic data at A_{420} were collected and rates determined by fitting to a one-exponential, pseudo-first-order function. Each datum is the average of three to five shots, with the standard deviation shown as a vertical bar. A similar experiment conducted with a different sGC preparation is shown in Figure S1 of the Supporting Information. The averages and standard deviations of k_{on} and k_{off} values determined from four different batches of the sGC preparation are 1.0 ± 0.3 μM^{-1} s^{-1} and 27 ± 4 s^{-1}, respectively.

labeled 5c NO–sGC complex by greatly increasing its concentration at the second mixing.

The presence of a substantial amount of the same nitrogen isotope in the final 5c NO–sGC complex as in the NO ligand used for the second mixing convincingly demonstrates that the heme iron is the binding site for the second NO molecule. The occupancy of the final 5c NO–sGC complex by the isotope used in the second mixing increased from 43 to 85%, when the NO stoichiometry was increased from 1 to 10 relative to the level of heme. This increase is substantial, and such a large extent of isotope replacement of the bound NO ligand deserves a quantitative mechanistic interpretation (see below).

Insignificant Isotope Scrambling during the 5–10 s Period of Freeze Trapping. To maximize the amount of 6c NO–sGC complex, we need to use a rapid-mixing technique for the first-stage mixing to track a fast reversible binding step with a k_{on} of 4.5 × 10^8 M^{-1} s^{-1} and a k_{off} of 27 s^{-1} (k_1/k_{-1} in Table 1, and Scheme 1) to select the best delay time before the second-stage mixing. Although the 5c NO–sGC complex formed after the second NO mixing appeared to be stable for at least 1 min (Figure 1C), the 5–10 s freezing time of the sample after the second mixing may potentially contribute to some isotope scrambling. This event may occur because of a possible dissociation of NO from the projected transient bis-NO quaternary complex (C in Scheme 1), followed by the rebinding of NO with the other isotope label before the sample was completely frozen. To address whether such a scenario is possible, we had to carefully assess the kinetic destiny of the potential transient quaternary complex intermediate (complex C in Scheme 1). In our previous publication,[20] we determined the k_{on} and k_{off} values of these chemical steps (k_6/k_{-6} and k_7 listed in Table 1):

$$6\text{cFe(II)NO} + \text{NO} \leftrightarrow \text{Fe(II)(NO)}_2 \rightarrow 5\text{pFe(II)NO} \quad (\text{B} \leftrightarrow \text{C} \rightarrow \text{D in Scheme 1})$$

Our rapid-scan data revealed a direct conversion of 6cFe(II)-NO (with a 420 nm Soret peak) to either 5cFe(II)NO or 5pFe(II)NO (with a Soret peak at 399 nm) with no indication of any accumulation of Fe(II)(NO)$_2$ (Figure 1). The only reported bis-NO complex with heme was described for the model heme Fe(II)(TmTP) (TmTP = *meso*-tetra-*m*-tolyl-

dx.doi.org/10.1021/bi300105s | *Biochemistry* 2012, 51, 2737–2746

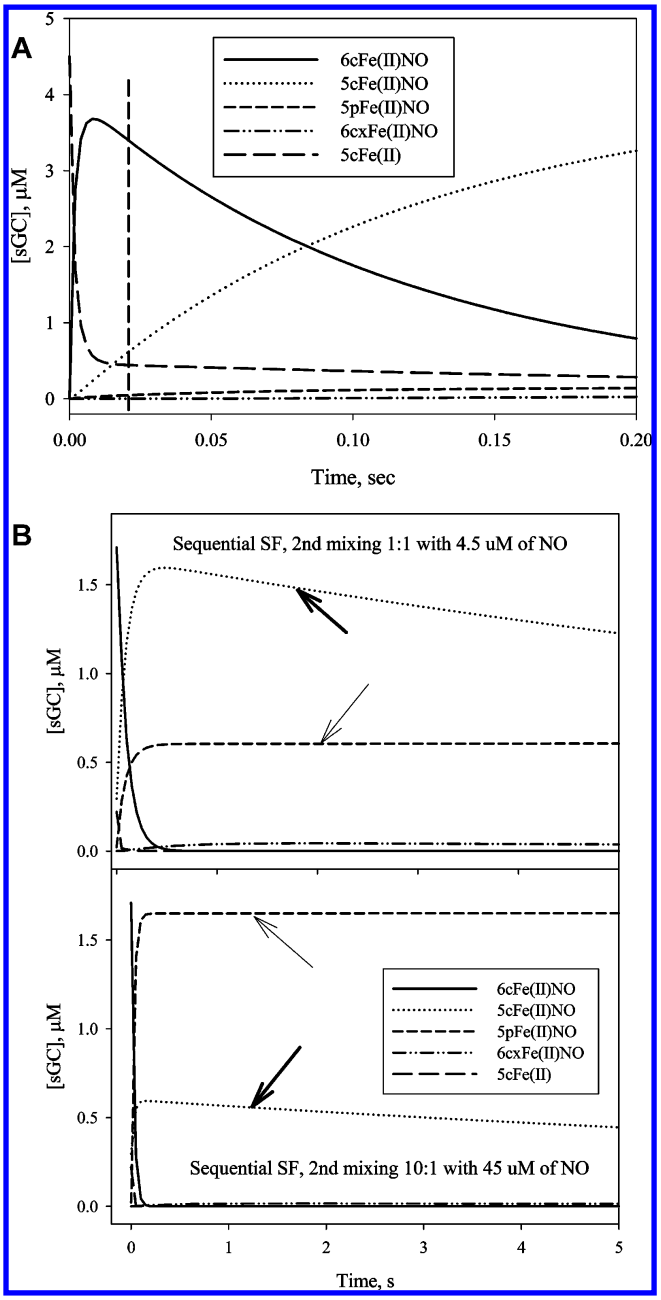

Figure 5. Simulation of the kinetics of 5cFe(II), 6cFe(II)NO, 5cFe(II)NO, 5pFe(II)NO, and 6cxFe(II)NO. Data were generated using the parameter values listed in Table 1. (A) The optimal aging time of ~20 ms for the formation of 6c Fe(II)NO in the first mixing (—) between 9 μM sGC and 10 μM NO is indicated by a vertical dashed line. (B) The time-dependent changes of various intermediates, especially those for the five-coordinate NO complexes: 5cFe(II)NO (···) and 5pFe(II)NO (---) indicated by thick and thin arrows, respectively, during a 5 s reaction after the second mixing with 5 μM (top) or 50 μM NO (bottom). Notice the large change in the relative ratio between 5cFe(II)NO and 5pFe(II)NO when the NO:sGC ratio is changed from 1:1 to 10:1 indicated by thick and thin arrows. The matching values of this ratio for individual freeze-trap EPR experiments shown in Figures 2 and 3 were derived by mathematical modeling and are listed in Table 2.

porphinato dianion) in organic solvents.[22] The Fe(II)(TmTP)-$(NO)_2$ complex exhibits a 416 nm Soret absorption peak, which is very different from that of the 5cFe(II)(TmTP)(NO) complex, 404 nm. This bis-NO was very transient and detected only at low temperatures.[22] These measurements for the bis-NO heme model strongly indicate that the spectrum of the putative bis-NO−sGC intermediate should be different from that of either the 5c or 6c NO−sGC complex. Thus, the observed single-stage optical conversion from 420 nm species to 399 nm species of the interaction of NO with sGC indicates that, if there is any formation of the bis-NO−sGC complex, it has to be very transient and very difficult to detect directly.

Two competing processes contribute to the depletion of Fe(II)$(NO)_2$ [k_{-6} and k_7 (Table 1)]. If $k_7 \gg k_{-6}$, negligible isotope scrambling is expected. However, if this condition is not satisfied, we expect that isotope scrambling will occur because of the faster dissociation of NO from Fe(II)$(NO)_2$ followed by the rebinding of NO with either isotope to 6c Fe(II)NO and the formation of the Fe(II)$(NO)_2$-containing NO ligands with a partly scrambled isotope label. Our studies showed that the observed rate of change of the 420 nm absorbance is linearly dependent on NO concentration, reaching ~600 s^{-1} at 900 μM NO and yielding a k_{on} (as the slope) of 0.6×10^6 M^{-1} s^{-1} and a k_{off} (as the y-intercept) of 26 s^{-1} (Figure 4 and Figure S1 of the Supporting Information, inset), consistent with our previous determination using concentrations of NO of <100 μM.[20] In this study, we pushed the measurements to the data acquisition limit of our stopped-flow instrument, with more than 50% of the reaction lost in the instrument's dead time (Figure S1 of the Supporting Information). Nonetheless, a linear dependence on NO concentration was still maintained, without any sign of saturation. Thus, we can safely conclude that the conversion from Fe(II)$(NO)_2$ to 5pFe(II)NO is at least 1 order of magnitude faster than the back dissociation reaction [i.e., $k_7 \gg k_{-6}$ (Table 1)], with little chance of observing the accumulation of the Fe(II)$(NO)_2$ intermediate. Consequently, there should be little concern about isotope scrambling during the 5−10 s freeze trapping phase of our kinetic measurements, and the level of 5pFe(II)NO is expected to plateau very rapidly, as observed in Figure 1C and predicted by computer modeling (see Figure 5).

To directly test if any scrambling of the NO ligand takes place in the 5c NO−sGC complex formed after the second mixing, we thawed the EPR samples from those shown in Figure 2 anaerobically and after incubation for 60 s at 24 °C refroze the samples and recorded the EPR spectra again (Figure S2 of the Supporting Information). We found minimal changes in the EPR spectra of each sample following these thaw−freeze cycles, strongly indicating that the five-coordinate Fe(II)NO samples reached a plateau during the thaw−freeze treatment, just as predicted by computer simulations (Figure 5B), and no additional ligand scrambling occurred. These results confirm that $k_7 \gg k_{-6}$, thus leading to a rapid plateau of the 5c NO−sGC species.

Concerted Mechanism for the Second Binding of NO to the Heme and Selective Dissociation of Distal NO from the Bis-NO Complex. Our recent kinetic study of the interaction of sGC with stoichiometric NO revealed the following multiphase transformation:[20]

$$\text{5cFe(II)}\ (430\ \text{nm}) \leftrightarrow \text{6cFe(II)NO}\ (420\ \text{nm})$$
$$(k_1/k_{-1},\ 4.5 \times 10^8\ M^{-1}\ s^{-1}/27\ s^{-1})$$

$$\text{6cFe(II)NO} \rightarrow \text{5cFe(II)NO}\ (399\ \text{nm})\ (\text{D}^*)$$
$$(k_2/k_{-2},\ 8.5\ s^{-1}/0.001\ s^{-1})$$

dx.doi.org/10.1021/bi300105s | Biochemistry 2012, 51, 2737−2746

$$5cFe(II)NO \rightarrow \{6cxFe(II)NO\}(E^*) \quad (k_3/k_{-3},\ 0.06\ s^{-1}/0\ s^{-1})$$

$$\{6cxFe(II)NO\} \rightarrow 5cxFe(II)\ (430\ nm) \quad (k_4/k_{-4},\ 2\ s^{-1}/0\ s^{-1})$$

$$5cxFe(II) \rightarrow 5cxFe(II)NO\ (399\ nm) \quad (k_5/k_{-5},\ 0.006\ s^{-1}/0\ s^{-1})$$

A simplified mechanism (A ↔ B → D* → E*) is presented in Scheme 1 (left), where 6cxFe(II)NO indicates a desensitized intermediate, which may contain an alternative proximal ligand such as His107. The value of k_2, the intrinsic rate constant for dissociation of the proximal histidine ligand (His105), was measured to be ∼10 s^{-1}, and subsequent chemical steps are at least 10-fold slower.[20]

When the interaction of NO and sGC occurs in the presence of excess NO, the binding of the second NO to the heme iron can follow either a sequential mechanism (i.e., His105 first dissociates, and then NO binds) or a concerted model (i.e., NO binding and His105 release occur simultaneously). If the sequential model is correct, then the rate of the the second binding of NO is limited by the intrinsic dissociation of His105 (∼10 s^{-1}). The experimental data presented in Figure 4 and Figure S1 of the Supporting Information, however, indicate that the second NO binding rate is linearly dependent on NO concentration up to >600 s^{-1}, with no indication of saturation. Thus, binding of the second NO molecule follows the concerted model, and a higher NO concentration facilitates the release of the His105 ligand. This finding and the lack of direct optical data for a bis-NO−sGC complex led us to introduce a quaternary bis-NO transition complex (C in Scheme 1) to indicate the fast concerted NO binding, His105 dissociation, and the subsequent discharge of the first NO ligand.

Because the rate of release of NO from $Fe(II)(NO)_2$ is ≫600 s^{-1} and cannot be rate-limiting in the whole sequence of the interaction of NO with sGC, the discharge of one NO ligand from $Fe(II)(NO)_2$ has to be selective for the distal site to avoid another efficient mechanism of isotope scrambling. If the NO release were to happen randomly from both axial positions, the final 5cFe(II)NO complex would contain equal parts of ^{14}NO and ^{15}NO ligands, independent of the concentration of the applied second NO isotope. However, we observed a preferential enrichment of the final 5cFe(II)NO with the increased concentration of the NO isotope used in the second mixing (Figure 2 vs Figure 3). Thus, the final stable 5c NO−sGC complex [5pFe(II)NO] has the NO ligated to the proximal position, similar to that observed for cytochrome *c*′, which is supported well by crystallographic, mutagenesis, resonance Raman spectroscopy, and geminate rebinding kinetic studies.[5,6,23,24]

Mathematical Modeling of the Interaction of NO with sGC. After characterizing the details of the binding of NO to sGC with either stoichiometric or excess NO, we performed mathematical modeling to assess the plausibility of our observed EPR data. The mechanistic model is proposed in Scheme 1, and the chemical steps involved are listed in Table 1. The rate constants applied in the simulation were either extracted from the literature or determined previously by us.[20,25] The mechanism for sGC reaction with stoichiometric NO is simplified in Scheme 1 by removing the k_4/k_{-4} and k_5/k_{-5} steps. These two chemical steps described and characterized in our recent study were included in the initial simulation, but their removal did not noticeably alter the predictions of the kinetic behavior of the 5c NO−sGC complex, which includes both 5cFe(II)NO and 5pFe(II)NO species with NO at the distal and proximal side of the heme, respectively. We first calculated the theoretical levels of 5cFe(II), 6cFe(II)NO, 5cFe(II)NO, and 5pFe(II)NO 20 ms after the first 1:1 mixing of sGC with NO (Figure 5A) and used these concentrations as starting values to simulate the reaction of the second-stage mixing (Figure 5B). The concentrations of two other species, 6cxFe(II)NO (a desensitized state that may contain an alternative proximal histidine) and $Fe(II)(NO)_2$ complex (E* and C, respectively, in Scheme 1), are essentially zero. Computer modeling indicates that at 20 ms, 3.4 μM of the 4.5 μM (i.e., 76%) total sGC is present as 6cFe(II)NO (420 nm peak), 0.59 μM is present as 5cFe(II)NO, 0.44 μM is present as 5cFe(II), and a small amount, 0.044 μM, is present as 5pFe(II)NO (Figure 5A, vertical dashed line). It was not possible to generate a pure 6c NO−sGC complex because of the fast back dissociation to the resting ferrous species (27 s^{-1}) and further conversion to the 5c NO−sGC complex (10 s^{-1} for B → D* in Scheme 1). Setting k_3 and/or k_5 to zero does not noticeably change the predicted level for 6cFe(II)NO at 20 ms, but setting k_2 to zero increases the level of 6cFe(II)NO to 4.0 μM and lowers the level of 5c Fe(II)NO for several seconds after the first mixing. In this case, the five-coordinate Fe(II)NO, exclusively 5pFe(II)NO, approached 3.8 and ∼4.5 μM at 2 s with 1× and 10× NO, respectively, in the second mixing (data not shown). This result shows that the kinetics of conversion from B to D* (Scheme 1) plays a key role in determining the amount and identity of 5c Fe(II)NO.

When the simulation was conducted on the basis of the reaction of sGC with a stoichiometric amount of NO at both stages of mixing, the predicted ratio of the levels for the two 5c NO−sGC complexes containing either ^{15}NO or ^{14}NO 5 and 10 s after the second mixing varied from 1.48 to 1.13 (Table 2),

Table 2. Observed and Predicted Levels for 5c NO−sGC Species Containing the Isotopic NO Used in the First- or Second-Stage Reaction in the Stopped Flow[a]

[NO] (first mixing) (μM)	[NO] (second mixing) (μM)	[5cFe(II)NO]:([5pFe(II)NO] + [5pFe(II)NO*] + [5cFe(II)NO*])[b] observed (EPR)	[5cFe(II)NO]:([5pFe(II)NO] + [5pFe(II)NO*] + [5cFe(II)NO*])[b] predicted (5−10 s) by simulation
10.0	5.0	1.2	1.48−1.13
10.0	5.0	1.3	1.48−1.13
15.0	7.5	0.75	1.02−0.76
10.0	50	0.18	0.24−0.16

[a]The sGC concentration was 4.5 μM for each reaction. [b]5cFe(II)NO* and 5pcFe(II)NO* are the 5c NO complexes derived from residual 5c Fe(II) after a 20 ms delay. Ratios are adjusted for binding of NO* to 5c Fe(II) to form 5cFe(II)NO* and 5pFe(II)NO* in the second-stage reaction.

which is comparable to the experimentally observed values of 1.2 and 1.3 (Figure 2A, B), independent of the order of isotope addition in the two mixing stages. These predicted values have been corrected for small contributions from the interaction of the isotopic NO in the second mixing with the small percentage of remaining free 5cFe(II)sGC predicted from computer

dx.doi.org/10.1021/bi300105s | *Biochemistry* 2012, 51, 2737−2746

simulation for the first stage reaction at 20 ms. With more than stoichiometric NO present for the first mixing (Figure 3A), the additional NO did not have much chance to attack the proximal side during the 20 ms aging, while the amount of NO with the opposite label used in the second mixing drove substantialy more displacement of the His105 ligand as predicted by our mechanistic model. This explains why we observed more conversion of the three-line EPR (NO at the distal side of the heme) to the two-line EPR (NO at the proximal side of the heme) when 15 μM ^{14}NO and 7.5 μM ^{15}NO were sequentially reacted with 9 μM sGC (Figure 3A). The observed ratio, 0.75, between two 5c NO−sGC complexes containing either ^{14}NO or ^{15}NO is close to the range predicted by simulation: 1.02−0.76 from 5 to 10 s after the second mixing (Table 2).

On the other hand, when sGC was first mixed with a stoichiometric amount of ^{14}NO followed by a 10-fold excess of ^{15}NO, we observed a ratio of 0.18 for the two 5c NO−sGC complexes containing ^{14}NO and ^{15}NO (Figure 3B), respectively, making 5pFe(II)NO the dominant species of the 5c NO−sGC complex. Our computer simulation predicted that this ratio varies from 0.24 to 0.16 from 5 to 10 s after the second mixing. Thus, the experimentally observed ratios for the two forms of the 5c NO−sGC complex are near the values predicted by simulations for the longer times, implying that the time to freeze trap the sample may be longer than we had anticipated and that it might take ∼8−10 s to completely freeze the reaction in all four experiments (Table 2). It should be noted that the ratio of these two types of 5c NO−sGC complexes is very sensitive to the rates of the reactions that branch out from 6cFe(II)NO, i.e., k_2/k_{-2} versus k_6/k_{-6}; thus, batch-to-batch variations in the sGC preparation showing some differences in the relative rates of these two steps might also cause a noticeable shift in the observed ratio.

In summary, using a sequential application of isotope-labeled NO with stoichiometric or excess amounts and freeze-quench EPR, we demonstrated for the first time that, provided with sufficient amounts of NO, the rapid interaction of NO with sGC includes the binding of the second NO molecule to the heme iron and not to other targets, such as cysteine thiol. These data predict that the rate of conversion from Fe(II)$(NO)_2$ to the 5c NO−sGC complex, i.e., 5pFe(II)NO, is >600 s^{-1} and overrides the back dissociation of NO, occurring at a respectable rate of 25 s^{-1}. The second NO ligates to the heme iron in concert with the dissociation of His105. Only the mechanism that considers the dissociation of NO from the distal and not the proximal position in the transient bis-NO complex, Fe(II)$(NO)_2$, is compatible with all previously published kinetic data for the interaction of NO with sGC. Our studies provide strong evidence of the heme proximal site being the site of binding of the second NO. Finally, the two chemical steps that branch out from 6cFe(II)NO constitute a sensitive control of the ratio of the two types of 5c NO−sGC complexes. We confirmed that both types of 5c NO−sGC complexes show prominent activity of formation of cGMP and are important intermediates for sGC catalytic turnover.[20] Excess NO favors the formation of 5pFe(II)NO, a 5c NO−sGC species with NO ligated at the proximal site, which should be the key intermediate that contributes to the formation of cGMP during the steady-state catalysis of sGC when NO is in excess.

■ ASSOCIATED CONTENT

Supporting Information

Additional NO binding kinetics (main panel) and the linear NO concentration dependence (inset) (Figure S1) and EPR obtained from samples shown in panels A and B of Figure 2 (a and c) after anaerobic thawing at 24 °C for 1 min and refreezing (Figure S2). This material is available free of charge via the Internet at http://pubs.acs.org.

■ AUTHOR INFORMATION

Corresponding Author

*A.-L.T.: Department of Internal Medicine, Division of Hematology, The University of Texas Medical School at Houston, Houston, TX 77030; telephone, (713) 500-6771; fax, (713) 500-6810; e-mail, ah-lim.tsai@uth.tmc.edu. E.M.: Department of Internal Medicine, Division of Cardiology, The University of Texas Medical School at Houston, Houston, TX 77030; telephone, (713) 486-3442; fax, (713) 486-0450; e-mail, emil.martin@uth.tmc.edu.

Funding

This work was supported by National Institutes of Health Grants HL088128 (E.M.) and HL095820 (A.-L.T.).

Notes

The authors declare no competing financial interest.

■ ACKNOWLEDGMENTS

We thank Professor Graham Palmer for his careful reviewing of the manuscript and John S. Olson for his fruitful discussions.

■ ABBREVIATIONS

GTP, guanosine triphosphate; cGMP, 3′,5′-cyclic guanosine monophosphate; sGC, soluble guanylyl cyclase; TEA, triethanolamine; 5c, five-coordinate; 6c, six-coordinate; NO, nitric oxide; ^{15}NO, NO containing ^{15}N; ^{14}NO, NO containing ^{14}N; EPR, electron paramagnetic resonance spectrometry; RFQ, rapid-freeze quench; Fe(II), ferrous form; 5cFe(II), five-coordinate ferrous sGC; 6cFe(II)NO, 6c NO−sGC complex; 5cFe(II)NO, 5c NO−sGC complex with NO at the heme distal site; Fe(II)$(NO)_2$, transient quaternary complex containing bis-NO heme; 5pFe(II)NO, 5c NO−sGC complex with NO at the heme proximal site; 6cxFe(II)NO, 6c NO−sGC complex in the desensitized state, possibly containing His107 as an alternative proximal ligand; 5cxFe(II), desensitized 5c ferrous sGC possibly containing His107 as an alternative proximal ligand.

■ REFERENCES

(1) Zhao, Y., Schelvis, J. P., Babcock, G. T., and Marletta, M. A. (1998) Identification of histidine 105 in the β1 subunit of soluble guanylate cyclase as the heme proximal ligand. *Biochemistry 37*, 4502−4509.

(2) Poulos, T. L. (2006) Soluble guanylate cyclase. *Curr. Opin. Struct. Biol. 16*, 736−743.

(3) Derbyshire, E. R., and Marletta, M. A. (2009) Biochemistry of soluble guanylate cyclase. *Handb. Exp. Pharmacol.*, 17−31.

(4) Zhao, Y., Brandish, P. E., Ballou, D. P., and Marletta, M. A. (1999) A molecular basis for nitric oxide sensing by soluble guanylate cyclase. *Proc. Natl. Acad. Sci. U.S.A. 96*, 14753−14758.

(5) Lawson, D. M., Stevenson, C. E., Andrew, C. R., and Eady, R. R. (2000) Unprecedented proximal binding of nitric oxide to heme: Implications for guanylate cyclase. *EMBO J. 19*, 5661−5671.

(6) Hough, M. A., Antonyuk, S. V., Barbieri, S., Rustage, N., McKay, A. L., Servid, A. E., Eady, R. R., Andrew, C. R., and Hasnain, S. S.

(2011) Distal-to-proximal NO conversion in hemoproteins: The role of the proximal pocket. *J. Mol. Biol. 405*, 395−409.
(7) Russwurm, M., and Koesling, D. (2004) NO activation of guanylyl cyclase. *EMBO J. 23*, 4443−4450.
(8) Sayed, N., Baskaran, P., Ma, X., van den Akker, F., and Beuve, A. (2007) Desensitization of soluble guanylyl cyclase, the NO receptor, by S-nitrosylation. *Proc. Natl. Acad. Sci. U.S.A. 104*, 12312−12317.
(9) Russwurm, M., and Koesling, D. (2004) Guanylyl cyclase: NO hits its target. *Biochem. Soc. Symp.*, 51−63.
(10) Cary, S. P., Winger, J. A., Derbyshire, E. R., and Marletta, M. A. (2006) Nitric oxide signaling: No longer simply on or off. *Trends Biochem. Sci. 31*, 231−239.
(11) Fernhoff, N. B., Derbyshire, E. R., and Marletta, M. A. (2009) A nitric oxide/cysteine interaction mediates the activation of soluble guanylate cyclase. *Proc. Natl. Acad. Sci. U.S.A. 106*, 21602−21607.
(12) Kharitonov, V. G., Sundquist, A. R., and Sharma, V. S. (1995) Kinetics of nitrosation of thiols by nitric oxide in the presence of oxygen. *J. Biol. Chem. 270*, 28158−28164.
(13) Martin, E., Berka, V., Tsai, A.-L., and Murad, F. (2005) Soluble guanylyl cyclase: The nitric oxide receptor. *Methods Enzymol. 396*, 478−492.
(14) Feelisch, M., and Noack, E. A. (1987) Correlation between nitric oxide formation during degradation of organic nitrates and activation of guanylate cyclase. *Eur. J. Pharmacol. 139*, 19−30.
(15) Wu, G., Lu, J. M., van der Donk, W. A., Kulmacz, R. J., and Tsai, A.-L. (2011) Cyclooxygenase reaction mechanism of prostaglandin H synthase from deuterium kinetic isotope effects. *J. Inorg. Biochem. 105*, 382−390.
(16) Tsai, A.-L., Berka, V., Kulmacz, R. J., Wu, G., and Palmer, G. (1998) An improved sample packing device for rapid freeze-trap electron paramagnetic resonance spectroscopy kinetic measurements. *Anal. Biochem. 264*, 165−171.
(17) Tsai, A.-L., Berka, V., Martin, F. E., Ma, X., van den Akker, F., Fabian, M., and Olson, J. S. (2010) Is *Nostoc* H-NOX an NO sensor or redox switch? *Biochemistry 49*, 6587−6599.
(18) Wei, C., Kulmacz, R. J., and Tsai, A.-L. (1995) Comparison of branched-chain and tightly coupled reaction mechanisms for prostaglandin H synthase. *Biochemistry 34*, 8499−8512.
(19) Tsai, A.-L., Berka, V., Martin, E., and Olson, J. S. (2012) A "Sliding-Scale Rule" for Selectivity between NO, CO and O_2 by Heme Protein Sensors. *Biochemistry 51*, 172−186.
(20) Tsai, A.-L., Berka, V., Sharina, I., and Martin, E. (2011) Dynamic ligand exchange in soluble guanylyl cyclase: Implications for sGC regulation and desensitization. *J. Biol. Chem. 286*, 43182−43192.
(21) Makino, R., Matsuda, H., Obayashi, E., Shiro, Y., Iizuka, T., and Hori, H. (1999) EPR characterization of axial bond in metal center of native and cobalt-substituted guanylate cyclase. *J. Biol. Chem. 274*, 7714−7723.
(22) Lorkovic, I. M., and Ford, P. C. (2000) Nitric Oxide Addition to the Ferous Nitrosyl Porphyrins Fe(P)(NO) Gives trans-Fe(P)$(NO)_2$ in Low-Temperature Solutions. *J. Am. Chem. Soc. 122*, 6516−6517.
(23) Andrew, C. R., Green, E. L., Lawson, D. M., and Eady, R. R. (2001) Resonance Raman studies of cytochrome c′ support the binding of NO and CO to opposite sides of the heme: Implications for ligand discrimination in heme-based sensors. *Biochemistry 40*, 4115−4122.
(24) Kruglik, S. G., Lambry, J. C., Cianetti, S., Martin, J. L., Eady, R. R., Andrew, C. R., and Negrerie, M. (2007) Molecular basis for nitric oxide dynamics and affinity with *Alcaligenes xylosoxidans* cytochrome c. *J. Biol. Chem. 282*, 5053−5062.
(25) Kharitonov, V. G., Sharma, V. S., Magde, D., and Koesling, D. (1997) Kinetics of nitric oxide dissociation from five- and six-coordinate nitrosyl hemes and heme proteins, including soluble guanylate cyclase. *Biochemistry 36*, 6814−6818.
(26) Martin, E., Berka, V., Bogatenkova, E., Murad, F., and Tsai, A.-L. (2006) Ligand selectivity of soluble guanylyl cyclase: Effect of the hydrogen bonding tyrosine in the distal heme pocket on binding of oxygen, nitric oxide and carbon monoxide. *J. Biol. Chem. 281*, 27836−27845.
(27) Brandish, P. E., Buechler, W., and Marletta, M. A. (1998) Regeneration of the ferrous heme of soluble guanylate cyclase from the nitric oxide complex: Acceleration by thiols and oxyhemoglobin. *Biochemistry 37*, 16898−16907.
(28) Kharitonov, V. G., Russwurm, M., Magde, D., Sharma, V. S., and Koesling, D. (1997) Dissociation of nitric oxide from soluble guanylate cyclase. *Biochem. Biophys. Res. Commun. 239*, 284−286.